

Indian Journal of Pure & Applied Physics  
Vol. 55, August 2017, pp. 541-550

## Spectroscopic investigations, DFT computations and other molecular properties of 2,4-dimethylbenzoic acid

E Gobinath<sup>a\*</sup>, S Jeyavijayan<sup>a</sup> & R John Xavier<sup>b</sup>

<sup>a</sup>Department of Physics, Kalasalingam University, Krishnankoil 626 126, India

<sup>b</sup>PG and Research Department of Physics, Periyar EVR College, Tiruchirappalli 620 023, India

Received 14 July 2016; accepted 3 January 2017

The molecular vibrations of 2,4-dimethylbenzoic acid (DMBA) have been investigated by recording Fourier transform infrared (FTIR) and FT-Raman spectroscopy. The complete vibrational assignment and analysis of the fundamental modes of the compound have been carried out using the experimental data and quantum chemical studies from DFT calculations employing MPW1PW91 and B3LYP methods employing 6-311++G(d,p) basis set. The <sup>1</sup>H and <sup>13</sup>C NMR chemical shifts have been calculated with the GIAO method using the optimized parameters obtained from B3LYP/6-311+G(d,p) method. Important thermodynamic properties and electronic properties have been calculated. Low value of HOMO-LUMO energy gap suggests the possibility of intramolecular charge transfer in the molecule. Furthermore, the first hyperpolarizability and total dipole moment of the molecule have been calculated.

**Keywords:** 2,4-dimethylbenzoic acid, FTIR, FT-Raman, NMR, MPW1PW91, B3LYP

### 1 Introduction

Benzoic acid is the most commonly used chemical standard to determine the heat of capacity of a bomb calorimeter. It inhibits the growth of mold, yeast, some bacteria and used in the treatment of fungal skin diseases such as tinea, ringworm, and athlete's foot<sup>1</sup>. The products based on benzoic acid have a long history of use as topical antiseptics and inhalant decongestants. Benzoic acids and their salts are permitted food preservatives in many types of foods<sup>2</sup> and their derivatives are used in medicine as a protective drug against UV radiation, in the diagnosis of gastrointestinal disorders and therapeutically in fibrotic skin disorders<sup>3</sup>. Substituted benzoic acids are very important materials in chemical and pharmaceutical industries and can be prepared by oxidation of the corresponding substituted toluene<sup>4</sup>. A patent reported that, their activity being related to novel synergistic compositions that selectively control tumor tissue<sup>5</sup>. The interesting features of benzoic acids and their derivatives have dragged the researchers from many fields to take up research and considerable amount of researches have been made in the field of spectroscopy too<sup>6,7</sup>. But to the best of our knowledge neither quantum chemical calculations nor the vibrational spectroscopic study of 2,4-dimethylbenzoic acid (DMBA) has been carried out.

The scarce of literature and attractive features of substituted benzoic acid motivated us to take up the detailed vibrational spectroscopic investigation of the title compound.

Density functional theory (DFT) methods lead to the prediction of more accurate molecular structure and vibrational frequencies of polyatomic molecules than the conventional *ab initio* Hartree-Fock calculations<sup>8</sup>. DFT approaches, using hybrid functional have evolved into a powerful and very reliable tool, being routinely used for the determination of various molecular properties. B3LYP functional has been previously shown to provide an excellent compromise between accuracy and computational efficiency of vibrational spectra for large and medium size molecules<sup>9,10</sup>. Further, Barone and Adamo's<sup>11</sup> Becke-style one parameter functional using the modified Perdew-Wang exchange<sup>12</sup> and Perdew-Wang 91 correlation method (MPW1PW91) are the best in predicting results for molecular geometry and vibrational wave numbers for moderately larger molecule.

### 2 Experimental Details

The fine polycrystalline sample of DMBA was purchased from commercial sources and they were used as such without further purification. The room temperature Fourier transform infrared spectra of the title compound was measured in the region 4000-400

\*Corresponding author (E-mail: [gobinath03@yahoo.co.in](mailto:gobinath03@yahoo.co.in))

$\text{cm}^{-1}$  at a resolution of  $\pm 1 \text{ cm}^{-1}$  using a JASCO FTIR-6300 spectrometer. KBr pellets were used in the spectral measurements. The FT-Raman spectrum of the title compound was recorded on a BRUKER RFS 100/S model interferometer equipped with FRA-106 FT-Raman accessory in the Stokes region  $3500\text{--}50 \text{ cm}^{-1}$  using the  $1064 \text{ nm}$  line of Nd:YAG laser for excitation, operating at  $150 \text{ mW}$  power. The reported wave numbers are believed to be accurate within  $\pm 4 \text{ cm}^{-1}$ .

### 3 DFT Calculations

Density functional theoretical computations involving two different methods namely MPW1PW91 and B3LYP for DMBA were performed by using Gaussian 09W program package<sup>13</sup> with 6-311++G(d,p) basis set to derive the complete geometry optimization. The molecular structure of the title compound in the ground state is computed by performing both the methods. The optimized structural parameters are used in the vibrational frequency calculations. Initial geometry generated from the standard geometrical parameters was optimized without any constraint on the potential energy surface at MPW1PW91 level adopting the standard 6-311++G(d,p) basis set. This geometry was then re-optimized again at DFT level employing the B3LYP method<sup>14</sup> using the correlation function of Lee *et al.*<sup>15</sup> implemented with the same basis set for better description of the bonding properties. All the parameters were allowed to relax and all the calculations converged to an optimized geometry which corresponds to a true minimum and the absence of the imaginary frequencies are ensured. The Cartesian representation of the theoretical force constants have been computed at the fully optimized geometry. In order to have better agreement with the experimental data, the multiple scaling of the force constants were performed according to SQM procedure<sup>16</sup> using relative scaling in the natural internal coordinate representation<sup>17</sup>. Further, the important thermodynamic properties of the title compound, electronic properties which are related to spectral activities have been theoretically computed by MPW1PW91 and B3LYP methods using 6-311++G(d,p) basis set.

## 4 Results and Discussion

### 4.1 Molecular geometry and structural properties

The molecular structure along with numbering of the atoms of DMBA is shown in Fig. 1. The global

minimum energies obtained by MPW1PW91 and B3LYP methods with 6-311++G(d,p) basis set for DMBA are calculated as  $-499.4621$  and  $-499.4846$  Hartrees, respectively. The optimized geometrical parameters of DMBA obtained by using the above methods are presented in Table 1 along with the experimental X-ray diffraction data<sup>18</sup>. It is found that the computed geometries using MPW1PW91 and B3LYP are consistent with each other as well as with the observed values.

### 4.2 Vibrational analysis

The molecule under investigation is having 21 atoms. Since it is considered to possess  $C_s$  point group symmetry, the 57 normal modes are distributed amongst the symmetry species as:

$$\Gamma_{\text{DMBA}} = 37A' (\text{in-plane}) + 20A'' (\text{out-of-plane})$$

Vibrational spectral assignments were performed on the recorded FT-IR and FT-Raman spectra based on the theoretically predicted wavenumbers by MPW1PW91 and B3LYP levels using 6-311++G(d,p) basis set and are presented in Table 2. None of the predicted vibrational spectra has imaginary frequencies. The observed FTIR and FT-Raman spectra of DMBA are presented in Figs 2 and 3, respectively. The calculated frequencies are usually higher than the corresponding experimental quantities, due to the combination of electron correlation effects and basis set deficiencies. After applying the scaling factors, the theoretical calculations reproduce the experimental data in well agreement.

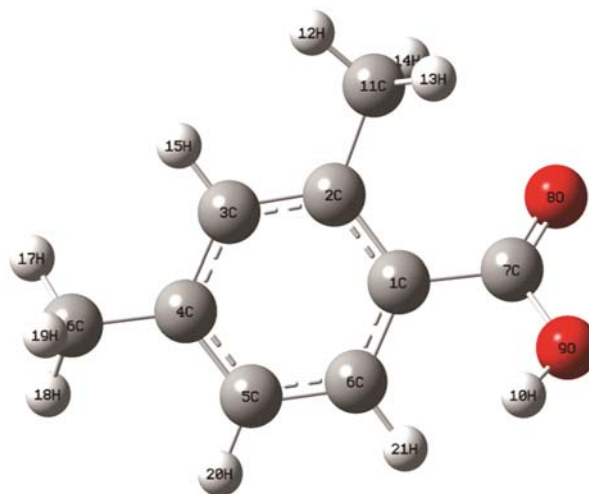


Fig. 1 — Molecular structure of 2,4-dimethylbenzoic acid along with numbering of atoms.

Table 1 — Experimental (XRD) and optimized geometrical parameters of 2,4-dimethylbenzoic acid obtained by MP1PW91 and B3LYP methods (*contd.*)

Parameters	Experimental <sup>a</sup>	MP1PW91/	B3LYP/
		6-311G++(d,p)	6-311++G(d,p)
Bond length (Å)			
C1 – C2	1.402	1.407	1.415
C1 – C6	1.376	1.400	1.405
C1 – C7	-	1.492	1.498
C2 – C3	1.365	1.393	1.401
C2 – C11	-	1.501	1.511
C3 – C4	1.377	1.394	1.401
C3 – H15	-	1.086	1.088
C4 – C5	1.407	1.393	1.401
C4 – C16	-	1.501	1.510
C5 – C6	1.382	1.386	1.397
C5 – H20	-	1.084	1.087
C6 – H21	-	1.086	1.087
C7 – O8	1.234	1.199	1.210
C7 – O9	1.312	1.354	1.367
O9 – H10	0.820	0.961	0.968
C11 – H12	-	1.091	1.093
C11 – H13	-	1.091	1.094
C11 – H14	-	1.091	1.094
C16 – H17	-	1.091	1.094
C16 – H18	-	1.091	1.094
C16 – H19	-	1.094	1.097
Bond angle (°)			
C1 – C2 – C3	120.8	117.75	117.77
C2 – C3 – C4	121.8	123.06	123.12
C3 – C4 – C5	117.1	118.12	118.06
C4 – C5 – C6	121.5	120.14	120.20
C1 – C6 – C5	120.2	121.27	121.30
C2 – C1 – C6	118.5	119.62	119.53
C2 – C1 – C7	120.7	120.76	120.81
C6 – C1 – C7	120.7	119.58	119.64
C1 – C2 – C11	-	122.83	122.94
C3 – C2 – C11	-	119.42	119.29
C2 – C3 – H15	-	118.21	118.18
C4 – C3 – H15	-	118.73	118.70
C3 – C4 – C16	-	120.71	120.80
C5 – C4 – C16	-	121.16	121.13
C4 – C5 – H20	-	120.06	120.06
C6 – C5 – H20	-	119.80	119.74
C1 – C6 – H21	-	119.90	119.92
C5 – C6 – H21	-	118.76	118.71
C1 – C7 – O8	123.4	124.70	124.76
C1 – C7 – O9	114.7	115.63	116.13
O8 – C7 – O9	121.8	119.67	119.10
C7 – O9 – H10	109.5	109.66	110.43
C2 – C11 – H12	-	110.23	110.22
C2 – C11 – H13	-	111.90	112.00
C2 – C11 – H14	-	110.84	110.97
H12 – C11 – H13	-	108.63	108.53

*(contd.)*

Table 1 — Experimental (XRD) and optimized geometrical parameters of 2,4-dimethylbenzoic acid obtained by MP1PW91 and B3LYP methods

Parameters	Experimental <sup>a</sup>	MP1PW91/	B3LYP/
		6-311G++(d,p)	6-311++G(d,p)
H12 – C11 – H14	-	108.86	108.77
H13 – C11 – H14	-	106.26	106.19
C4 – C16 – H17	-	111.41	111.45
C4 – C16 – H18	-	111.43	111.43
C4 – C16 – H19	-	110.62	110.79
H17 – C16 – H18	-	108.29	108.21
H17 – C16 – H19	-	107.39	107.36
H18 – C16 – H19	-	107.53	107.41

For numbering of atoms refers Fig. 1.

<sup>a</sup> Values are taken from Ref.<sup>18</sup>Table 2 — Experimental and calculated (unscaled and scaled) vibrational frequencies (cm<sup>-1</sup>), IR intensity (km mol<sup>-1</sup>), Raman intensity and probable assignments of 2,4-dimethylbenzoic acid using MP1PW91/6-311++G(d,p) and B3LYP/6-311++G(d,p) levels (contd.)

No.	Symm. Species C <sub>s</sub>	Experimental frequencies (cm <sup>-1</sup> )		MP1PW91/6-311++G(d,p)				B3LYP 6-311++G(d,p)				Characterization of normal modes with PED(%)
		FTIR	FT-Raman	Unscaled	Scaled	IR intensity	Raman intensity	Unscaled	Scaled	IR intensity	Raman intensity	
1.	A'	-	3221	3864	3239	40.99	1.05	3801	3227	32.44	1.54	vOH (99)
2.	A'	3078	3086	3204	3092	10.05	6.73	3192	3081	13.24	8.72	vCH (98)
3.	A'	-	3051	3182	3069	7.91	5.88	3172	3056	2.56	5.89	vCH (96)
4.	A'	3040	-	3180	3048	12.38	0.66	3171	3044	22.57	2.13	vCH (97)
5.	A'	2988	-	3150	2999	12.98	2.72	3129	2990	15.52	3.63	CH <sub>3</sub> ips (99)
6.	A'	2976	-	3146	2991	11.56	2.98	3124	2981	13.79	3.86	CH <sub>3</sub> ips (99)
7.	A'	2934	2936	3139	2948	5.83	3.15	3121	2939	7.20	4.09	CH <sub>3</sub> ss (98)
8.	A'	2883	-	3118	2896	12.94	4.22	3097	2887	16.20	5.52	CH <sub>3</sub> ss (98)
9.	A''	2813	-	3069	2827	15.13	10.35	3055	2819	19.33	12.11	CH <sub>3</sub> ops (96)
10.	A''	2739	-	3053	2751	19.90	14.92	3036	2744	25.19	17.96	CH <sub>3</sub> ops (96)
11.	A'	1690	-	1855	1708	363.51	13.5	1820	1696	344.19	18.36	vC=O (93)
12.	A'	1611	1611	1677	1628	52.95	14.99	1656	1617	51.92	19.72	vCC (84), bCC (13)
13.	A'	-	1573	1632	1591	11.67	3.63	1608	1579	10.60	4.58	vCC (85), bCH (12)
14.	A'	1497	-	1546	1521	10.03	1.56	1534	1499	7.02	2.54	CH <sub>3</sub> ipb (89)
15.	A'	1452	-	1500	1461	32.12	1.37	1499	1458	28.84	2.45	CH <sub>3</sub> ipb (89)
16.	A'	1437	-	1490	1452	6.38	3.21	1494	1442	7.19	4.34	vCC (80), CC (17)
17.	A'	1407	-	1487	1410	6.31	0.34	1491	1410	4.64	0.47	vCC (81), Rasynd (15)
18.	A'	-	1394	1479	1398	11.63	1.77	1483	1399	12.31	2.29	vCC (79), bCC (19)
19.	A'	-	1319	1438	1324	2.28	2	1433	1321	0.61	0.86	CH <sub>3</sub> sb (78)
20.	A'	1311	-	1420	1315	4.43	3.74	1426	1318	4.50	5.96	CH <sub>3</sub> sb (77)
21.	A'	-	1296	1413	1299	5.18	5.78	1420	1304	2.25	7.52	bOH (80), bCO (17)
22.	A'	1286	-	1363	1292	67.08	2.14	1345	1289	42.19	2.67	vCC (77), CC (21)
23.	A'	1279	-	1331	1290	449.90	5.11	1318	1283	29.76	1.34	vCO (82)
24.	A'	1272	-	1319	1276	2.64	0.55	1307	1271	426.93	4.82	vCC (80)
25.	A'	-	1265	1275	1267	8.15	9.63	1260	1262	20.91	12.89	vCC (74), Rasynd (17)
26.	A'	1235	1236	1224	1240	28.22	4.95	1213	1237	26.55	6.64	bC=O (73), bCC (13)
27.	A'	1187	-	1195	1192	2.20	1.9	1188	1188	5.62	3.4	vCC (80), Rtrigd (15)

(contd.)

Table 2 — Experimental and calculated (unscaled and scaled) vibrational frequencies ( $\text{cm}^{-1}$ ), IR intensity ( $\text{km mol}^{-1}$ ), Raman intensity and probable assignments of 2,4-dimethylbenzoic acid using MP1PW91/6-311++G(d,p) and B3LYP/6-311++G(d,p) levels

No.	Symm. Species $C_s$	Experimental frequencies ( $\text{cm}^{-1}$ )		MP1PW91/6-311++G(d,p)				B3LYP 6-311++G(d,p)				Characterization of normal modes with PED(%)
		FTIR	FT-Raman	Unscaled	Scaled	IR intensity	Raman intensity	Unscaled	Scaled	IR intensity	Raman intensity	
28.	A'	1158	-	1172	1165	7.26	1.92	11622	1160	6.25	0	bCO (72), bCC (13)
29.	A''	-	1094	1087	1099	55.02	1.6	1071	1097	59.92	1.7	CH <sub>3</sub> opb (80)
30.	A''	1089	-	1059	1093	10.54	0.08	1061	1090	10.33	0.13	CH <sub>3</sub> opb (78)
31.	A'	1041	-	1057	1045	1.57	0.07	1059	1043	2.64	0.27	Rasynd (72), CC (21)
32.	A'	-	939	1043	942	1.41	0.38	1042	942	1.88	0.39	Rtrigd (70), Rsymd (19)
33.	A'	930	-	1009	940	0.40	0.37	1010	937	0.51	0.64	CH <sub>3</sub> ipr (71)
34.	A'	916	-	975	932	0.30	0.12	967	920	0.26	0.19	CH <sub>3</sub> ipr (69)
35.	A'	-	892	958	915	4.21	3.84	947	899	4.39	4.72	bCH (68), Rasynd (21)
36.	A''	838	-	904	851	2.12	0.49	900	842	2.79	0.53	CH <sub>3</sub> opr (71)
37.	A''	-	821	847	836	13.35	0.18	839	825	15.94	0.3	CH <sub>3</sub> opr (70)
38.	A'	784	-	789	787	17.00	1.11	777	780	13.87	1.11	bCH (63), CC (23)
39.	A'	771	-	766	775	16.53	11.79	753	766	14.23	16.65	bCH (65), Rtrigd (19)
40.	A'	726	726	739	734	5.22	5.49	730	729	5.57	4.56	Rsymd (69), Rasynd (21)
41.	A'	692	-	712	704	7.12	0.9	704	698	7.09	1.12	bCC (63), bCO (17)
42.	A'	608	-	608	608	4.76	1.15	601	605	4.13	1.45	bCC (65), CC (23)
43.	A'	580	-	580	584	2.81	5.65	575	578	2.65	6.85	bCC (60), Rtrigd (19)
44.	A''	-	572	553	570	11.87	5.43	551	564	10.15	8.05	$\omega$ OH (59), $\omega$ CC (23)
45.	A''	-	-	519	513	71.47	1.31	513	508	72.11	1.61	$\omega$ CH (57), bCC (15)
46.	A''	-	-	501	496	12.87	4.05	501	485	13.57	4.91	$\omega$ CH (55), tRtrig (27)
47.	A''	-	-	443	472	4.91	0.3	443	469	4.09	0.35	$\omega$ CC (57), tRsym (25)
48.	A''	-	383	405	391	3.31	2.8	404	387	3.45	3.53	$\omega$ CH (60), $\omega$ CC (19)
49.	A''	-	294	343	303	1.07	9.91	341	298	1.11	12.55	$\omega$ CC (53), $\omega$ CO (23)
50.	A''	-	-	289	286	1.73	1.2	290	283	1.63	1.4	$\omega$ CC (55), tRsym (23)
51.	A''	-	-	255	253	6.06	7.72	256	250	6.24	10.08	$\omega$ CO (51), $\omega$ CC (23)
52.	A''	-	-	204	201	5.54	5.41	205	200	5.09	7.39	tRtrig (53), tRsym (27)
53.	A''	-	-	195	200	4.83	2.89	196	199	5.08	3.5	tRsym (51), $\omega$ CO (21)
54.	A''	-	123	156	132	0.61	3.44	154	128	0.57	4.86	$\omega$ CO (52), tRtrig (19)
55.	A''	-	-	92	104	0.92	28.8	93	99	0.98	32.06	tRsym (51), tRsym (21)
56.	A''	-	-	66	81	5.47	68.07	64	75	5.53	87.69	CH <sub>3</sub> twist (63)
57.	A''	-	-	37	46	0.19	100	42	50	0.19	100	CH <sub>3</sub> twist (61)

Abbreviations used :v-stretching; ss – symmetric stretching; b-bending;  $\omega$ -out-of-plane bending; R-ring; trigd-trigonal deformation; symd-symmetric deformation; asymd-antisymmetric deformation; t-torsion; s-strong; vs-very strong; ms-medium strong; w-weak; vw-very weak.

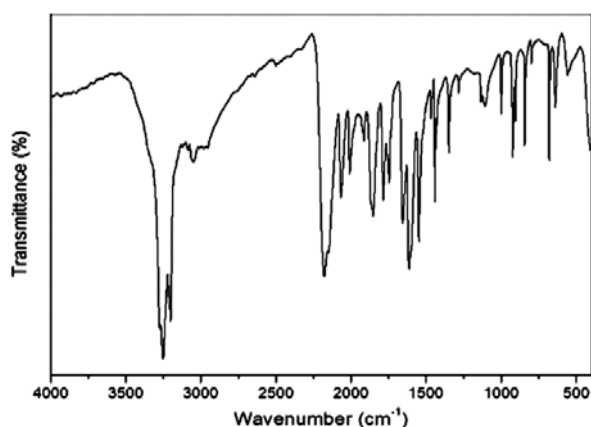


Fig. 2 — FTIR spectrum of 2,4-dimethylbenzoic acid.

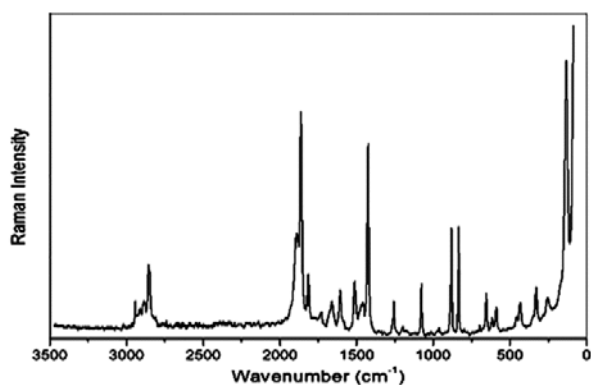


Fig. 3 — FT-Raman spectrum of 2,4-dimethylbenzoic acid.

#### 4.2.1 C-H vibrations

The hetero aromatic structure shows the presence of C–H stretching vibration in the region 3100–3000  $\text{cm}^{-1}$ , which is the characteristic region for the ready identification of C–H stretching vibration<sup>19</sup>. In DMBA, the scaled wavenumbers computed by MP1PW91 and B3LYP methods using 6-311++G(d,p) basis set at 3092, 3069, 3048  $\text{cm}^{-1}$  and at 3081, 3056, 3044  $\text{cm}^{-1}$ , respectively, are assigned to C–H stretching mode of vibrations with almost 100% PED. Similarly, the experimental IR and Raman bands of the title compound are found at 3078, 3040  $\text{cm}^{-1}$  and 3086 and 3051  $\text{cm}^{-1}$ , respectively. The wave numbers of other fundamental modes like C–H in-plane and C–H out-of-plane bending modes observed in DMBA are found to be consistent with the calculated wave numbers by MP1PW91 and B3LYP methods using 6-311++G(d,p) basis set as given in Table 2.

#### 4.2.2 CH<sub>3</sub> vibrations

Generally, nine fundamentals can be associated to each CH<sub>3</sub> group. They are namely, CH<sub>3</sub> asymmetric

stretch; CH<sub>3</sub> symmetric stretch; CH<sub>3</sub> in-plane bending; CH<sub>3</sub> symmetric bending; CH<sub>3</sub> in-plane rocking; CH<sub>3</sub> out-of-plane rocking and CH<sub>3</sub> twisting hydrogen bending modes. In addition to that, CH<sub>3</sub> out-of-plane stretch and the CH<sub>3</sub> out-of-plane bending modes of the CH<sub>3</sub> group which are expected to be depolarized for *A''* symmetry species. Methyl group vibrations are generally referred to as electron-donating substituent in the aromatic rings system, the antisymmetric C–H stretching mode of CH<sub>3</sub> is expected around 2980  $\text{cm}^{-1}$  and CH<sub>3</sub> symmetric stretching is expected<sup>20</sup> at 2870  $\text{cm}^{-1}$ . In the anti symmetric C–H stretching mode, the two C–H bonds of the methyl group are expanding while the third one is contracting. In the CH<sub>3</sub> symmetric stretching, all the three C–H bonds expand and contract in phase<sup>21</sup>. The IR active bands at 2988  $\text{cm}^{-1}$  and 2976  $\text{cm}^{-1}$  were assigned to CH<sub>3</sub> in-plane stretching mode of vibration for which the calculated wave numbers by MP1PW91 and B3LYP methods are 2999, 2991  $\text{cm}^{-1}$  and 2990 and 2981  $\text{cm}^{-1}$  with almost 100% contribution towards the total PED. The bands computed at 2948, 2896  $\text{cm}^{-1}$  and 2939 and 2887  $\text{cm}^{-1}$  have been assigned to CH<sub>3</sub> symmetric stretching for which the experimental bands are at 2934, 2936 and 2883  $\text{cm}^{-1}$ . For methyl substituted benzene derivatives, the anti symmetric and symmetric deformation vibrations of methyl group normally appear in the region 1465–1440  $\text{cm}^{-1}$  and 1390–1370  $\text{cm}^{-1}$ , respectively<sup>22</sup>. Accordingly, in DBMA, IR bands at 1497 and 1452  $\text{cm}^{-1}$  were assigned to CH<sub>3</sub> in-plane bending mode of vibrations. The bands at 1319 and 1311  $\text{cm}^{-1}$  have been assigned to CH<sub>3</sub> symmetric bending. The other fundamental vibration modes of CH<sub>3</sub> group are given in Table 2 and also found to be in good agreement with the calculated wave numbers by MP1PW91 and B3LYP methods using 6-311++G(d,p) basis set.

#### 4.2.3 COOH vibrations

The most characteristic feature of carboxylic group is a single band, which is observed usually in the range 1690–1655  $\text{cm}^{-1}$  region and this band is due to the C=O stretching vibration<sup>23</sup>. The IR bands computed at 1708 and 1696  $\text{cm}^{-1}$  and observed at 1690  $\text{cm}^{-1}$  in DMBA have been assigned to C=O stretching. Two other characteristic carboxylic group vibrations are: C–O stretching and O–H in-plane bending. They are expected in the range<sup>24</sup> of 1350–1200  $\text{cm}^{-1}$ . Generally, the C–O stretching mode appears at a lower frequency than the O–H in-plane

bending mode. In line with the above, the Raman band observed at  $1296\text{ cm}^{-1}$  is assigned to O–H in-plane bending mode and the IR band observed at  $1279$  is assigned to C–O stretching.

#### 4.3 Thermodynamic properties

The thermodynamic properties like heat capacity, entropy, rotational constants, dipole moment and zero point vibrational energy (ZPVE) of the title compound have been computed at 298.15 K and 1.00 atomic pressure by MPW1PW91 and B3LYP levels using 6-311++G(d,p) basis set and they are presented in Table 3. Table 4 gives the thermodynamic properties like standard heat capacities, standard entropies and the standard enthalpy changes of the title compound in gas phase at different temperatures calculated by B3LYP/6-311++G(d,p) method. Figure 4 depicts the correlation of heat capacity at constant pressure ( $C_p$ ), entropy ( $S$ ) and enthalpy changes ( $\Delta H_{0\rightarrow T}$ ) with temperature and it is observed that the

Table 3 — Theoretically computed thermodynamic parameters of 2,4-dimethylbenzoic acid

Parameter	2,4-dimethylbenzoic acid	
	MP1PW91	B3LYP
Zero-point vibrational energy (kJ/mol)	449.258	446.484
	2.20753	2.18069
Rotational constants (GHz)	0.76813	0.75864
	0.58995	0.58207
Thermal energy (kJ/mol)		
Total	114.080	113.435
Translational	0.889	0.889
Rotational	0.889	0.889
Vibrational	112.302	111.658
Molar capacity at constant volume ( $\text{cal mol}^{-1}\text{Kelvin}^{-1}$ )		
Total	39.420	39.640
Translational	2.981	2.981
Rotational	2.981	2.981
Vibrational	33.458	33.678
Entropy ( $\text{cal mol}^{-1}\text{Kelvin}^{-1}$ )		
Total	102.406	102.319
Translational	40.928	40.928
Rotational	30.153	30.191
Vibrational	31.325	31.200
Dipole moment (Debye)		
$\mu_x$	-4.7694	-4.850
$\mu_y$	-1.0813	-1.1477
$\mu_z$	1.4016	1.4087
$\mu_{\text{total}}$	5.0873	5.1796

thermodynamic functions are increasing with temperature since the molecular vibrations increase with temperature. The corresponding fitting equations with fitting factors ( $R^2$ ) are as follow:

$$S_m^\circ = 1.42884 \times 10^{-5} T^2 + 0.1183 T + 57.6177 \quad (R^2 = 0.9999)$$

Table 4 — Thermodynamic properties at different temperatures of 2,4-dimethylbenzoic acid

$T$ (K)	$S_m^\circ$ ( $\text{cal mol}^{-1}\text{K}^{-1}$ )	$C_p$ ( $\text{cal mol}^{-1}\text{K}^{-1}$ )	$\Delta H_m^\circ$ ( $\text{kcal mol}^{-1}$ )
100	69.21735	19.09532	10.94242
200	82.08936	30.2137	18.30526
298.15	94.46673	41.6027	27.50914
300	94.5159	41.6027	27.50914
400	107.1728	52.45193	37.8795
500	120.1848	61.83937	49.11793
600	133.567	69.60724	61.05106
700	147.2992	76.00434	73.55803
800	161.3476	81.32861	86.54512
900	175.6751	85.8146	99.93656
1000	190.2464	89.63074	113.6704

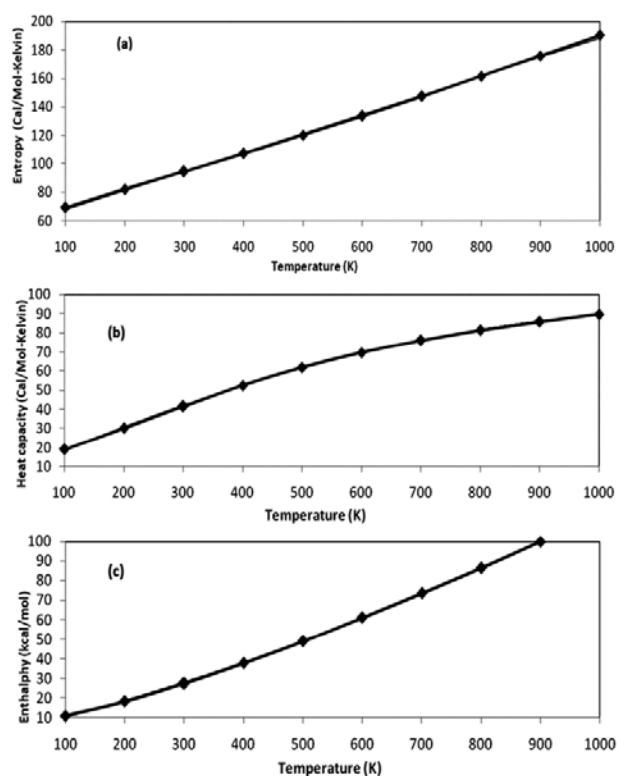


Fig. 4 — Correlation graph for for 2,4-dimethylbenzoic acid (a) entropy and temperature (b) heat capacity and temperature, and (c) enthalpy and temperature.

$$C_p^\circ = -5.65792 \times 10^{-5} T^2 + 0.1412 T + 4.8565 \quad (R^2 = 0.9996)$$

$$\Delta H_m^\circ = 3.6182 \times 10^{-5} T^2 + 0.0761 T + 2.0278 \quad (R^2 = 0.9997)$$

#### 4.4 NPA charge distribution

Since the charge distribution on the molecule has an important influence on the vibrational spectra, the natural population analysis (NPA) charge distributions of DMBA were calculated by MPW1PW91 and B3LYP methods using 6-311++G(d,p) basis set and jointly presented in Table 5. From the NPA values listed in Table 5, one can find the electropositive nature in all hydrogen atoms and two oxygen atoms are exhibiting electro negativity. But the carbon atoms are exhibiting electro positivity as well as electro negativity depending upon the nature of atoms bonded with them. From the Table 5, it can be seen that the atom C7 in DMBA is exhibiting electro positivity since it is connected to much more electronegative atoms O8 and O9.

#### 4.5 First hyperpolarizability

The potential application of the title compound in the field of nonlinear optics (NLO) demands the investigation of its structural and bonding features contributing to the hyperpolarizability enhancement, by

analyzing the vibrational modes using IR and Raman spectroscopy. Many organic molecules, containing conjugated electrons are characterized by large values of molecular first hyperpolarizability<sup>25</sup>. In this study, the B3LYP/6-311++G(d,p) method has been used for the prediction of first hyperpolarizability. First hyperpolarizability is a third rank tensor that can be described by  $3 \times 3 \times 3$  matrix. The 27 components of 3D matrix can be reduced to 10 components due to the Kleinmann symmetry<sup>26</sup>. The components of the first hyperpolarizability can be calculated using the following equations:

$$\beta = \beta_x^2 + \beta_y^2 + \beta_z^2$$

where,

$$\beta_x = \beta_{xxx} + \beta_{xyy} + \beta_{xzz}$$

$$\beta_y = \beta_{yyy} + \beta_{xxy} + \beta_{yzz}$$

$$\beta_z = \beta_{zzz} + \beta_{xxz} + \beta_{yyz}$$

Urea is one of the prototypical molecules used in the study of the NLO properties of molecular systems. Therefore it is used frequently as a threshold value for comparative purposes. The calculated value of  $\beta$  for DMBA is  $1.943 \times 10^{-30}$  esu. Since the first hyperpolarizability of the DMBA is relatively much higher than that of Urea ( $\beta$  of urea is  $0.3728 \times 10^{-30}$  esu), the title compound possesses considerable NLO properties.

#### 4.6 <sup>1</sup>H and <sup>13</sup>C NMR chemical shifts

The isotropic chemical shifts are frequently used as an aid in identification of reactive organic as well as ionic species<sup>27</sup>. The Gauge-including atomic orbital (GIAO) <sup>1</sup>H and <sup>13</sup>C chemical shift calculations of the title compound has been made on the optimized geometry using B3LYP/6-311++G(d,p) method and are presented in Table 6. The <sup>1</sup>H NMR is interesting

Table 5 — The NPA charge distribution of 2,4-dimethylbenzoic acid

Atom	MP1PW91	B3LYP
C1	-0.18423	-0.18293
C2	0.02796	0.02167
C3	-0.20433	-0.22639
C4	-0.00142	-0.00843
C5	-0.21519	-0.23813
C6	-0.18962	-0.21538
C7	0.78789	0.80034
O8	-0.56415	-0.57587
O9	-0.67252	-0.70927
H10	0.47516	0.50610
C11	-0.60980	-0.67538
H12	0.20472	0.22940
H13	0.22695	0.24885
H14	0.24179	0.26257
H15	0.20669	0.23629
C16	-0.60559	-0.67392
H17	0.21690	0.23987
H18	0.21441	0.23881
H19	0.22286	0.24444
H20	0.21136	0.23997
H21	0.21017	0.23739

Table 6 — The <sup>1</sup>H and <sup>13</sup>C NMR shift (GIAO method) for 2,4-dimethylbenzoic acid

Atom	Chemical shift (ppm)	Atom	Chemical shift (ppm)
H10	8.94	C1	147.15
H12	7.66	C2	208.43
H13	11.33	C3	166.32
H14	8.23	C4	210.26
H15	9.62	C5	163.82
H17	7.42	C6	180.52
H18	7.62	C7	91.49
H19	7.87	C11	28.60
H20	7.24	C16	42.39
H21	7.88		



since the hydrogen atom is the smallest of all atoms and its chemical shift will be more susceptible to intermolecular interactions. The chemical shifts of all the protons have been calculated in between 7.24 ppm to 9.62 ppm where as the atom H13 is found to be the most deshielded with a chemical shift of 11.33 ppm. The typical range of  $^{13}\text{C}$  NMR chemical shift in organic molecules is greater<sup>28</sup> than 100 ppm. From the Table 6, the chemical shifts of carbon atoms in methyl group namely C11 and C16 are found to be most shielded among carbon atoms and have the chemical shifts of 28.60 and 42.39 ppm, respectively.

#### 4.7 Frontier molecular orbital analysis

The highest occupied molecular orbit (HOMO) is the orbital that primarily acts as an electron donor and the lowest unoccupied molecular orbit (LUMO) is the orbital that largely acts as the electron acceptor. The MOs are defined as Eigen functions of the Fock operator, which exhibit the full symmetry of the nuclear point group and they necessarily form a basis for irreducible representations of full point-group symmetry<sup>29</sup>. The interaction between the filled (HOMO) and unfilled (LUMO) orbitals are giving the stability to the structure. Further, the energy gap between HOMO and LUMO has been used to prove the bioactivity from intra-molecular charge transfer<sup>30</sup> (ICT). The energies of important frontier orbitals (FMOs) such as HOMO, LUMO, LUMO+1 and HOMO-1 and their orbital energy gaps are calculated using B3LYP/6-311++G(d,p) method and the pictorial illustration of the FMOs of DMBA have been given in Fig. 5. In DMBA, the HOMO is located

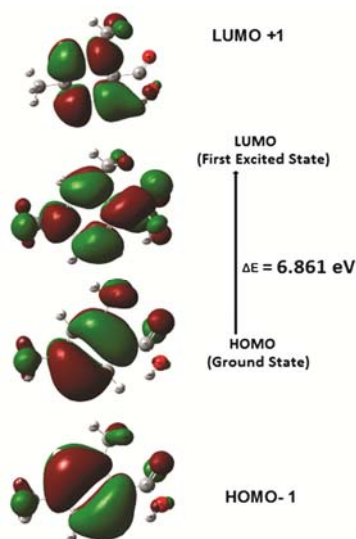


Fig. 5 — Plots of the frontier orbitals of 2,4-dimethylbenzoic acid.

over  $\text{CH}_3$  groups and LUMO: of  $\pi$  nature, (i.e., benzene ring) is delocalized over the whole C-C bond and COOH group; consequently the HOMO→LUMO transition implies an electron density transfer to the C–C bond of the benzene ring and COOH group from  $\text{CH}_3$  groups. Moreover, these orbitals significantly overlap in their position for DMBA. But, while the HOMO-1 is localized on the benzene ring, LUMO+1 is localized on almost the whole molecule. Both the HOMOs and the LUMOs are mostly  $\pi$ -anti-bonding type orbitals. In DMBA, there are 40 occupied molecular orbitals. The energy gap between HOMO and LUMO is found to be 6.861 eV. The energy gap of HOMO–LUMO explains the eventual charge transfer interaction within the molecule, which influences the biological activity of the molecule. Furthermore, the decrease in energy gap between HOMO and LUMO facilitates intra molecular charge transfer which makes the material to be NLO active.

## 5 Conclusions

The optimized structure of the title compound 2,4-dimethylbenzoic acid has been obtained and the bond length and bond angles for the optimized structure have been computed using MPW1PW91 and B3LYP methods with 6-311++G(d,p) basis set. The calculated geometric parameters are found to be consistent with the observed values. The vibrational frequencies of the fundamental modes of the compound have been precisely assigned with the help of recorded FTIR and FT-Raman spectra. From the NMR chemical shifts, the hydrogen attached or nearby electron withdrawing atom or group can decrease the shielding whereas the methyl group increases the shielding. NPA analysis has been made to determine the charge distribution on the molecule. From the thermodynamic properties, it is seen that the heat capacities, entropies and enthalpies increase with the increasing temperature owing to the intensities of the molecular vibrations increase with increasing temperature. The energy gap of HOMO–LUMO explains the eventual charge transfer interaction within the molecule, which influences the biological activity of the molecule. The first hyperpolarizability calculations show that the title molecule possesses considerable NLO properties.

## References

- 1 Warth A D, *Appl Environ Microbiol*, 57 (1991) 3410.
- 2 Pollard J A, Russel N J & Gould G W, *Food preservatives*, (AVI Publishers: New York), (1991) 235.
- 3 Swinslocka R, Samsonowicz M, Regulaska E & Lewandowski W, *J Mol Struct*, 792 (2006) 227.

- 4 Sheldon R A & Kochi J K, *Metal-catalyzed oxidations of organic compounds*, (Academic: New York), 1981.
- 5 Kreutz K & Schlossberg A, *US Patent* 6,395,720 B1 (2002).
- 6 Karabacak M & Cinar M, *Spectrochim Acta*, 86A (2012) 590.
- 7 Karabacak M, Cinar Z, Kurt M, Sudha S & Sundaraganesan N, *Spectrochim Acta*, 85A (2012) 179.
- 8 Ramalingam S & Periandy S, *Spectrochim Acta*, 78A (2011) 835.
- 9 Korth H G, De Heer M I & Mulder P, *J Phys Chem*, 106 (2002) 8779.
- 10 Xavier R J & Gobinath E, *Spectrochim Acta*, 91A (2012) 248.
- 11 Adamo C & Barone V, *J Chem Phys*, 108 (1998) 664.
- 12 Burke K, Perdew J P, Wang Y, Dobson J F, Vignale G & Das M P, *Electronic density functional theory: Recent progress and new directions*, (Plenum Press: New York), 1998.
- 13 Frisch M J, Trucks G W & Schlegel H B, *Gaussian 09, Revision A 02*, (Gaussian, Inc: Wallingford CT), 2009.
- 14 Becke A D, *J Chem Phys*, 98 (1993) 5648.
- 15 Lee C, Yang W & Parr R G, *Phys Rev*, B37 (1998) 785.
- 16 Rauhut G & Pulay P, *J Phys Chem*, 99 (1995) 3093.
- 17 Fogarasi G & Pulay P & Doring J R, *Vibrational spectra and structure*, (Elsevier: Amsterdam), 1985.
- 18 Arshad M N, Tahir M N, Khan I U, Shafiq M & Waheeda A, *Acta Crystallogr*, E65 (2009) 0640.
- 19 Jeyavijayan S, *Indian J Pure Appl Phys*, 54 (2016) 269.
- 20 Sajan D, Hubert Joe I & Jayakumar V S, *J Raman Spectrosc*, 37 (2005) 508.
- 21 Karabacak M, Cinar Z, Kurt M, Sudha S & Sundaraganesan N, *Spectrochim Acta*, 85A (2012) 179.
- 22 Areanas J F, Tocn I L, Otero J C & Marcos J I, *J Mol Struct*, 410 (1997) 443.
- 23 Socrates G, *Infrared and raman characteristic group frequencies*, (John Wiley: New York), 2001.
- 24 Coates J, *Interpretation of infrared spectra, a practical approach*, in Meyers R A (Eds), *Encyclopedia of analytical chemistry*, (John Wiley & Sons Ltd: Chichester), 2000.
- 25 Karpagam J, Sundaraganesan N, Sebastian S, Manoharan S & Kurt M, *J Raman Spectrosc*, 41 (2010) 53.
- 26 Kleinman D A, *Phys Rev*, 126 (1962) 1977.
- 27 Sebastian S, Sundaraganesan N, Karthikeyan B & Srinivasan V, *Spectrochim Acta*, 78A (2011) 590.
- 28 Kalinowski H O, Berger S & Brawn S, *Carbon <sup>13</sup> NMR spectroscopy*, (John Wiley and Sons: Chichester), 1988.
- 29 Petrucci R H, Harwood W S, Herring F G & Madura J D, *General chemistry: Principles & modern applications*, 9<sup>th</sup> Eds, (Pearson Education Inc: New Jersey), 2007.
- 30 Padmaja L, Ravi Kumar C, Sajan D, Hubert Joe I, Jayakumar V S & Pettit G R, *J Raman Spectrosc*, 40 (2009) 419.